SGP-TR-151-46

PROCEEDINGS

TWENTY-FIRST WORKSHOP GEOTHERMAL RESERVOIR ENGINEERING

January 22-24, 1996

Stanford Geothermal Program
Workshop Report SGP-TR-151

DISCLAIMER

PROCEEDINGS, Twenty-First Workshop on Geothermal Reservoir Engineering
Stanford University, Stanford, California, January 22-24, 1996
SGP-TR-151

HYDROLOGIC CHARACTERIZATION OF FOUR CORES FROM THE GEYSERS CORING PROJECT

Peter Persoff[1] and Jeffrey B. Hulen[2]

[1]Earth Sciences Division, Lawrence Berkeley National Laboratory, University of California, Berkeley CA 94720
[2]Earth Sciences and Resources Institute, Department of Civil and Environmental Engineering, University of Utah, Salt Lake City, UT 84112

ABSTRACT

Results of hydrologic tests conducted on four representative core plugs from Geysers Coring Project drill hole SB-15-D have been related to detailed mineralogic and textural characterization of the plugs to yield new information about permeability, porosity, and capillary-pressure characteristics of the uppermost Geysers steam reservoir and its immediately overlying caprock. The core plugs are all fine- to medium-grained, Franciscan-assemblage (late Mesozoic) metagraywacke with sparse Franciscan metamorphic quartz-calcite veins and late Cenozoic, hydrothermal quartz-calcite-pyrite veins. The matrices of three plugs from the caprock are rich in metamorphic mixed-layer illite/smectite and disseminated hydrothermal pyrite; the reservoir plug instead contains abundant illite and only minor pyrite. The reservoir plug and one caprock plug are sparsely disrupted by latest-stage, unmineralized microfractures which both follow and crosscut veinlets but which could be artifacts. Porosities of the plugs, measured by Boyles-law gas expansion, range between 1.9 and 2.5%. Gas permeability and Klinkenberg slip factor were calculated from gas-pressure-pulse-decay measurements using a specially designed permeameter with small (2 mL) reservoirs. Matrix permeabilities in the range 10^{-21} m^2 (= 1 nanodarcy) were measured for two plugs that included mineral-filled veins but no unfilled microfractures. Greater permeabilities were measured on plugs that contained microfractures; at 500 psi net confining pressure, an effective aperture of 1.6 μm was estimated for one plug. Capillary pressure curves were determined for three cores by measuring saturation as weight gain of plugs equilibrated with atmospheres in which the relative humidity was controlled by saturated brines.

INTRODUCTION

In support of The Geysers Coring Project, a collaborative effort involving the Department of Energy's Geothermal Division, Unocal Corporation and other Geysers steamfield operators, a team of collaborating investigators has been assembled to characterize porosity, permeability, remaining fluid saturation, and other hydrologic parameters (Hulen et al., 1995). The drilling phase of the project was successfully completed late in 1994, utilizing a sidetrack to an existing Unocal production well SB-15-D, in the northwest-central Geysers. The core was field-characterized and several sample suites (including the one utilized for the present study) were collected and variously preserved on site for distribution to the research team. In practical terms, the team's collective effort is aimed at providing new reservoir information to enable The Geysers' operating companies to prolong significantly the field's productive life.

For this investigation, we have determined the permeabilities, porosities, and capillary-pressure curves for representative plugs of four core runs from SB-15-D -- three from the portion of the drill hole believed to penetrate The Geysers' relatively impermeable caprock; the fourth from the immediately underlying steam reservoir. These hydrologic data are interpreted in the light of corresponding, detailed petrographic analyses of the plugs to provide additional information about the nature of The Geysers resource.

PERMEABILITY MEASUREMENT BY PRESSURE-PULSE DECAY

Steady-state measurement of very low permeability is limited by the need to measure very small flow rates. In the unsteady pressure-pulse-decay method, reservoirs up-and downstream of the sample are initially at different pressures, and the pressures in the up- and downstream reservoirs respectively fall and rise as fluid flows through the sample. Flow rates are not measured but inferred from the changes in pressure. Analytical solutions for gas-pressure-pulse-decay (GPPD) were derived by Ning (1993).

The apparatus used in these measurements, constructed following the design of Ning (1993), is shown in Figure 1. Sample plugs, 25 mm in

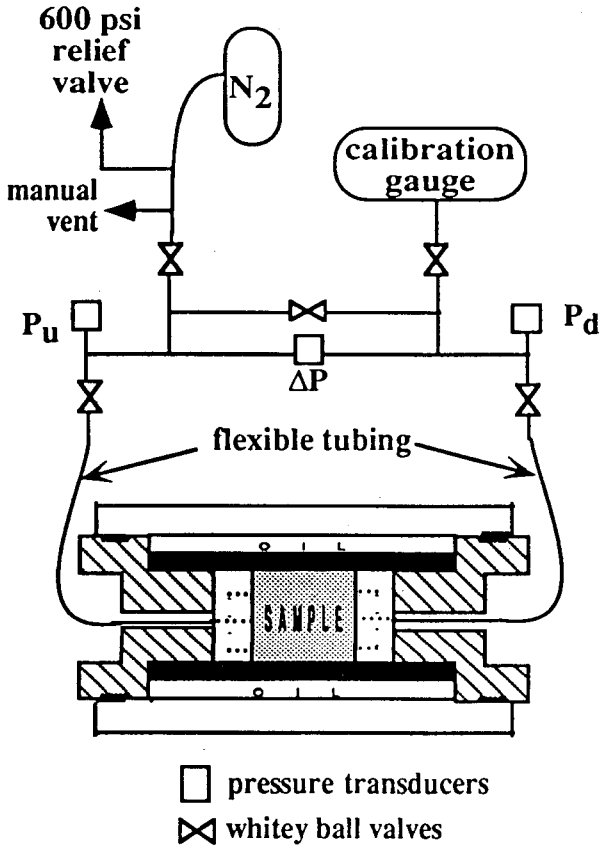

Figure 1. Gas-pressure-pulse-decay apparatus.

diameter and 50 mm long, were dried at 60°C to constant weight to avoid desiccating the clays. The sample holder was a Temco (Tulsa, OK) Hassler cell. Confining pressure of 500 psi above the initial upstream pressure was maintained by hydraulic oil around the rubber sleeve. To take advantage of the GPPD method, the up-and downstream reservoirs must be small. The system was therefore constructed using 1.6-mm o.d. and smaller stainless steel tubing for the reservoirs. Flexible stainless steel tubing with 0.8 mm o.d. and 0.25 mm i.d. was welded through the distribution plugs so that samples could be changed without breaking and remaking connections. As a result, most of the reservoir volume is contained in the valves, transducers, and fitting. A further advantage of using small i.d. tubing for the reservoir is that because of the large o.d./i.d. ratio, the compliance of the system is small. Validyne DP-15 transducers (Validyne, Anaheim, CA) were used to measure the upstream and downstream pressures (differential to ambient pressure), and the differential pressure. The difference between the upstream and downstream pressures served as a check on the differential pressure measurement. The volumes of the up-and downstream reservoirs were calculated from gas expansion tests into known volumes. The volume of the reservoirs calculated from these measurements was 2.2 mL in both the up- and downstream reservoirs. Temperature was controlled between 26.6 and 26.7°C.

A typical test is shown in Figure 2. The upstream pressure decreases before the downstream pressure starts to increase, because the pore space of the sample must be pressurized above its initial value to its final value. A rigorous interpretation of the data is possible by using the solutions of Ning (1993), which require numerical inversion of Laplace transforms; or by fitting the data with a numerical model of gas flow. Finsterle and Pruess (1995) have developed a simulator, ITOUGH, which does the inversion automatically, eliminating the need to guess permeability and other parameters. A less rigorous interpretation of the data was used in this work, in which the compressibility of the gas and the storage capacity of the sample were ignored. This reduces the problem to a simple falling-head permeability test, in which the differential pressure between the two reservoirs, ΔP, decays exponentially with time. Under these assumptions, and with the specification that the two reservoirs are of equal volume V, the permeability is calculated as

$$k = \frac{VM\mu L\left(\frac{d(\ln \Delta P)}{dt}\right)}{2RT\rho A} \qquad (1)$$

where k is the permeability, M and μ the molecular weight and viscosity of the gas, L and A are the sample length and cross-sectional area, ΔP is the t is time, and ρ is the density of the gas at the average pressure.

Figure 3 replots the data of Figure 2 to show that the data conform to the simplified model. In some tests, the assymetry noted in Figure 2 resulted in a slight curvature in the plot of ln ΔP against time.

Klinkenberg Factor. In gas flow, when the mean free path of the molecules approaches the pore size (i.e., when a significant fraction of molecular collision are with the pore wall rather than with other gas molecules), gas permeability is enhanced by "slip flow." Slip flow is important at low pressures and in small pores, and for the latter reason would therefore be expected to be significant in these plugs. We correct for this phenomenon by extrapolating the measured gas permeability to infinite pressure according to this equation (Klinkenberg 1941):

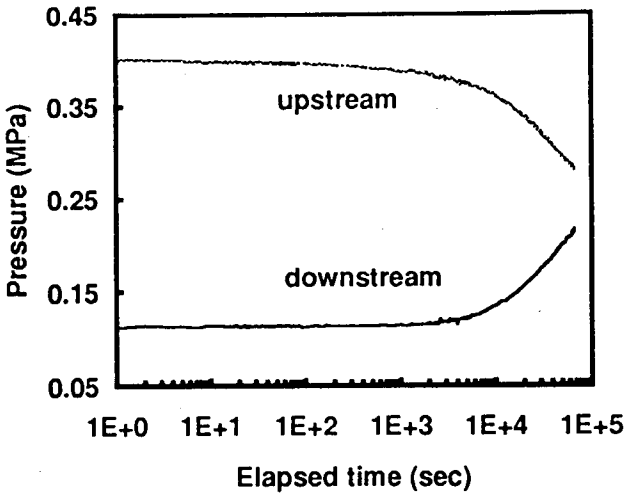

Figure 2. Pulse decay data for unfractured plug 54-1.

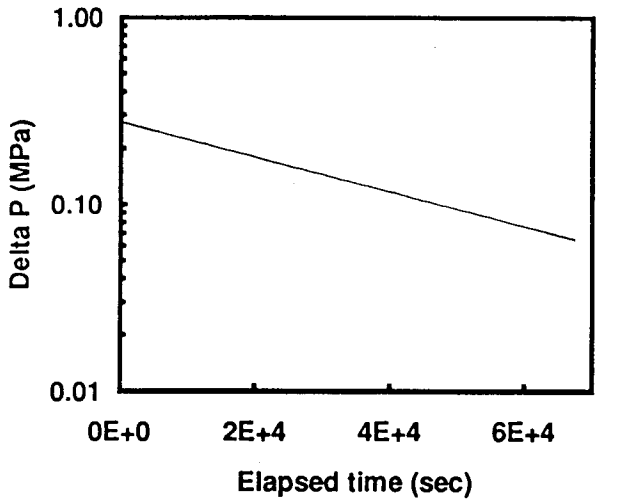

Figure 3. Data of Fig. 2 replotted. Data shown are measured ΔP.

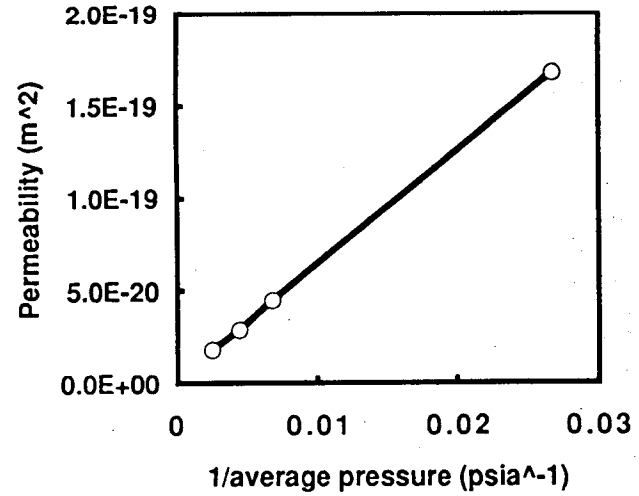

Figure 4. Klinkenberg plot of measured permeabilities for plug 26-2.

$$k_m = k\left(1+\frac{b}{\bar{p}}\right) \qquad (2)$$

where k_m is the measured permeability enhanced by slip flow, b is the Klinkenberg constant characteristic of the porous medium, and $\bar{p}$ is the average of the up- and downstream pressures. GPPD measurements were conducted on each plug at three or four pressures to permit extrapolation according to Eq. (2), as shown in Figure 4. Good linearity permitted extrapolation in all data sets. The Klinkenberg correction was derived from a steady-state analysis and uses the average values of the up- and downstream pressures. In these tests, because the up- and downstream reservoirs are of equal volume, the average pressure is almost constant (see Figure 2 for example), which allows the Klinkenberg plot to be used. To check the acceptability of the assumptions used in the calculation of permeability by Eq. (1), the data from one set of three runs at different pressures were simultaneously inverted using ITOUGH. The values of k and b obtained by this inversion were 1% and 5% less, respectively, than the values calculated by Eq. (1) and extrapolation as shown in Figure 4.

CAPILLARY PRESSURE CURVE MEASUREMENT BY VAPOR PRESSURE LOWERING.

The measurement of the capillary pressure curve by vapor pressure lowering combines two phenomena (Calhoun et al., 1949; Ward and Morrow, 1987; Pruess and O'Sullivan, 1992). The first is the Young-Laplace law, which relates the curvature of the meniscus in the pores of a partially saturated sample to the capillary pressure:

$$P_c \equiv P_G - P_L = \frac{2\sigma cos(\alpha)}{r} \qquad (3)$$

where P_C is the capillary pressure, P_G and P_L are the pressures in the gas and liquid phases, σ is the surface tension, r is the average radius of curvature of the meniscus, and α is the contact angle in the liquid phase. In small pores, Eq. (3) says that the pressure in the liquid phase may be negative, i.e., it is under tension.

The second phenomenon is the Kelvin equation, which relates the capillary pressure to a reduction in vapor pressure of water:

$$\frac{P_v}{P_{wo}} = exp\left(\frac{-M_w P_c}{\rho_w RT}\right) \qquad (4)$$

where P_V is the vapor pressure of water in the

atmosphere, P_{vo} is the saturation vapor pressure of water over a flat surface of pure water, M_w and ρ_w are the molecular weight and density of liquid water, R is the gas-law constant, and T is the absolute temperature. The ratio on the left side of Eq. (4) is the relative humidity, which is thus related to the capillary pressure. When a porous sample is in equilibrium with air of a specified humidity, all pores of radius smaller than that specified by Eq. (3) are filled with water.

Pruess and O'Sullivan (1992) point out that a corollary of the exponential relationship in the Kelvin equation is that a small reduction in the vapor pressure is equivalent to a great increase in capillary pressure. This makes it possible to achieve capillary pressures by vapor-pressure lowering that exceed capillary pressures that can be reached by any other method, including centrifuge methods.

A reduced vapor pressure of water (i.e., $P_v < P_{vo}$) was maintained in these experiments by equilibration of the atmosphere with saturated brine solutions. Glass desiccators, in an incubator at 28.5¤C, were used as the test chambers. Saturated solutions of nine salts were placed in the bottom of each chamber to control the humidity. The vapor pressures over these solutions are shown in Table 1, interpolated between the data points measured by Acheson (1965).

Three rock cores, from runs 15, 26, and 86, were used for these experiments. Six plugs (labeled -u through -z), 1.3 cm in diameter and 2.5 cm long, were cut from each core, and dried to constant weight at 60°C to avoid desiccating the clays. The plugs were equilibrated in various chambers, and cycled through several chambers of increasing, and then decreasing, humidity as shown in Table 1, while changes in saturation were monitored as weight gain. Although we follow the convention of treating saturation as the independent variable in the capillary pressure curve, in this experiment the capillary pressure is actually controlled independently by the vapor pressure of water in the chamber, and the saturation is measured as weight gain.

RESULTS

Table 2 summarizes the mineralogical observations from examination of the core plugs and thin sections and XRD, and the porosity and permeability data.

For plug 15-2, the calculated permeability was to large to represent matrix permeability, so it was converted to an effective aperture (Persoff and Pruess, 1995). Essentially, the sample is treated as a rectangle of width w equal to the actual fracture width (the diameter of the cylinder in this case) and height $h = \pi r^2/w$ to give the same cross sectional area. Then the effective aperture is

$$z = \sqrt[3]{12kh} \qquad (5)$$

For sample 15-2, the permeability was 2.20±0.02 x 10^{-16} m^2, from which z =1.6 μm.

Also, measurements at three average pressures all gave the same value of permeability. That is, the Klinkenberg constant b was approximately zero, and slip flow was not significant for this sample. This is consistent with the mean free path, 9.3 x 10^{-8} m or less, being much smaller than the aperture.

Table 1. Humidity history of plugs in vapor-pressure-lowering experiment.

Chamber	1	2	3	4	5	6	7	8	9
Satd. brine	$CaCl_2$	$MgCl_2$	NaI	KI	$SrCl_2$	NaCl	KBr	KCl	$Sr(NO_3)_2$
P_V (mbar)	10.1	12.7	14.4	26.7	27.3	29.5	30.1	31.5	31.5
rel. hum.	0.257	0.325	0.366	0.681	0.695	0.752	0.768	0.803	0.803
P_C (MPa)	189.2	156.5	139.8	53.5	50.5	39.6	36.7	30.6	30.5
-u	*1	2		3		4, 6		5	
-v		1	2		3		4, 6		5
-w		6	1	2, 5		3		4	
-x			6	1	2, 5		3		4
-y			5	4, 6	1	2		3	
-z	6		5		4	1	2		3

*Numerals in italics indicate the order in which each group of three plugs were placed in each chamber.

Table 2. Measured properties of plugs from SB-15D cores.

Core plug		15-2	26-2	54-1	86-2
Depth (m below ground)		290	319	393	482
Porosity, %	mean	2.2	1.9	----	1.9
	std dev of 6 plugs	0.5	0.2	----	0.5
Matrix permeability (10^{-21} m^2)		----	1.3	2.0	26
Effective fracture aperture, μm		1.6	n a	n a	n a
Klinkenberg b (psi)		----	390	3050	58.6
Veins, vol %		1.0 H 0.5 M	0.2 H 0.2 M	0.9 H 0.1 M	0.5 H 3.0 M
Late microfractures		yes	no	no	yes
Mineral and other constituents, wt. %	quartz	38	40	41	39
	albite	24	22	21	23
	K-feldspar	3	3	2	4
	calcite	3	n d	2	3
	epidote	n d	n d	tr	1
	wairakite	n d	n d	1	tr
	ilmenite	1	1	1	1
	sphene	2	2	2	2
	pyrite	3	4	4	1
	coarse muscovite	3	2	3	3
	illite	n d	n d	n d	12
	mixed layer illite/ smectite	15	16	14	n d
	chlorite	7	9	9	10
	organic debris	1	1	tr	1
Expandable interlayers in illite/smectite, %		5-10	5-10	5-10	n d

*H = geysers hydrothermal veins (late Cenozoic)
M = Franciscan metamorphic veins (late Mesozoic)
n d = not detected n a = not applicable
tr = trace ---- = not determined

Table 3. Values of constants to fit capillary-pressure curves to Eq. (6).

plugs	direction	a	b
15	wetting	11.35	-1.60
15	drying	13.55	-1.55
26	wetting	21.93	-1.89
26	drying	23.50	-2.11
86	wetting	10.28	-1.69
86	drying	10.23	-1.93

A typical pair of capillary-pressure curves, for the wetting and drying directions, is shown in Figure 5. The values of constants to fit the data to the form

$$P_c = aS^b \qquad (6)$$

where P_c is in MPa and S is a fraction, are shown in Table 3.

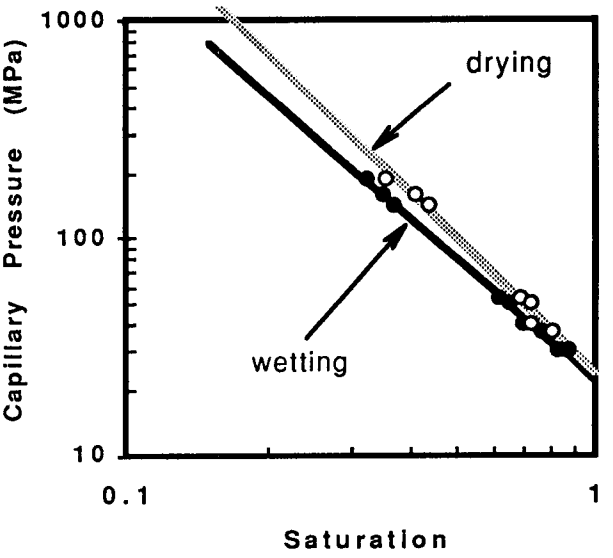

Figure 5. Capillary pressure curve for plugs from core 26

LITHOLOGY, VEIN MINERALIZATION, AND FRACTURING

Corehole SB-15-D, a sidetrack from SB-15, penetrated, in the depth range 251-488 m, 237 m of new, continuous core from an apparently monotonous sequence of Franciscan-Assemblage (late Mesozoic) metagraywackes and minor interstratified metashales or argillites (Hulen et al., 1995). The four cores collected from this sequence and utilized for our investigation are all metagraywackes -- three from the interpreted cap on the steam field; the fourth and deepest from the underlying, uppermost steam reservoir (Table 2). Although superficially similar, the cores have subtle mineralogic and textural features which help explain variations in corresponding measured hydrologic properties.

All four cores are fine- to medium-grained, massive to very vaguely planar-laminated, lithic metagraywacke consisting of angular to subrounded clastic grains (averaging about 0.4 mm in diameter) of intermediate- to basic-composition metavolcanic rock, quartz, albite, chert, coarse muscovite, and argillite, embedded in a matrix of illite (reservoir) or mixed-layer illite/smectite (caprock), chlorite, and "rock flour" compositionally identical to the clastic grains. These rocks are very poorly sorted, with the fine-grained matrix material effectively clogging what might otherwise be pores between the larger clastic grains. Layer silicates (illite, illite/smectite, and chlorite), including those in the matrix as well as those partially replacing some clastic grains (for example, chlorite after primary or metamorphic mafic minerals in metavolcanic clasts) account for a fairly consistent 22-25 wt% of these rocks (Table 2). Clastic ilmenite (and/or magnetite) and organic debris as well as secondary sphene are ubiquitous minor components of the cores.

The cores are weakly to moderately hydrothermally altered. Rock-forming albite is weakly and locally altered to potassium feldspar (adularia) and illite (or illite/smectite) in all the cores, but sparsely to the calc-silicates epidote and wairakite only in the two deeper ones. Disseminated hydrothermal pyrite accounts for 3-4% of the caprock cores, but only 1% of the reservoir core 86-2. (Table 2). Illite without detectable smectite interlayers is present only in this reservoir core. In the caprock cores, it is supplanted by mixed-layer illite/smectite with 5-10% expandable interlayers. This difference reflects conversion of illite/smectite (probably Franciscan metamorphic in origin) to illite in response to downward-increasing paleotemperature during circulation of the late Cenozoic, hot-water-dominated geothermal system which "dried out" to form the modern steam field (e.g. Hulen and Nielson, 1995; Moore and Gunderson, 1995).

Further evidence of this system is found in the thin (<2 mm wide) hydrothermal veins which occur sparsely in all four cores and are most abundant (est. 1 vol.%) in caprock core 15-2 (Table 2). These veins consist dominantly of quartz and calcite, with potassium feldspar, pyrite, wairakite, and mixed-layer illite/smectite (in the caprock samples) locally present. Also present in all four samples are older, metamorphic, Franciscan quartz-calcite veins. In some of these veins, the metamorphic calcite initially present has been dissolved, and the resulting voids infilled with the same secondary-mineral assemblage observed in The Geysers hydrothermal veins.

The youngest potential porosity/permeability elements in the cores are microfractures occurring both within (and parallel to) and crosscutting the veins in samples 15-2 and 86-2. These microfractures account for an estimated 0.3% of the volume of 15-2 and 0.1% of 86-2. They form anastamosing networks which are subparallel to the plug axes, with at least one microfracture exposed on each end of the two plugs. These microfractures are clearly extensional "pull-apart" features. Irregularities on a given microfracture wall have closely matching counterparts on the opposing wall. Apertures of the microfractures (at atmospheric pressure) range from <1 micron to (rarely) 200 microns; most apertures are <10 microns. These microfractures lack even traces of secondary mineralization which could serve to identify them as natural reservoir features. Because of the absence of such mineralization, these microfractures may be artifacts of well production, coring, or removal of the test plug from the core.

DISCUSSION

Fracture and matrix permeability. Host rocks for The Geysers geothermal field have both matrix and fracture permeability (e.g. Gunderson, 1990). Thus, one purpose of this work was to measure these two types of permeability in representative samples of the SB-15-D core. The three deeper plug samples, 26-2, 54-1, and 86-2, were chosen for measurement of matrix permeability, since even though they contained potentially permeable veins, none of these veins (or networks thereof) were throughgoing, that is, continuous from one end of the plug to the other. Sample 15-2, by contrast, contained a throughgoing hydrothermal vein, larger representatives of which are clearly the major porosity elements in the SB-15-D core (Hulen and Nielson, 1995). This sample, then was selected as a candidate for measurement of fracture permeability, since veins are really mineralized fractures, and if they are not totally filled by secondary minerals they remain partially open as potential fluid conduits.

Both the metamorphic and hydrothermal veins occurring in all the plugs studied (including 15-2) were shown petrographically to be fully filled fractures and thus impermeable. In both 15-2 and 86-2, however, the veins were partially rebroken by late stage microfractures. The higher permeabilities measured for these samples, therefore, can be attributed to these fractures. The permeabilities measured for the other two plugs can be considered true matrix permeability values. In the case of 86-2, the microfracture network increased the permeability only by one order of magnitude. In 15-2, however, the microfractures, including those developed in the throughgoing hydothermal veinlet, enhanced the permeability of the sample by five orders of magnitude (measured value 2.2×10^{-16} m^2 compared

to the matrix values). This fracture network was equivalent to a parallel plate fracture with an aperture of only 1.6 μm.

The Klinkenberg factor. The Klinkenberg slip factor *b* in Eq. 2 is a measure of how strongly slip flow influences the measured permeability. It has units of pressure but may be thought of as a measure inverse to the pore size. In tighter formations, therefore, *b* may be expected to be greater. Figure 6 shows this to be generally true, and the correlation found by Jones (1972) can be extended through four decades of permeability.

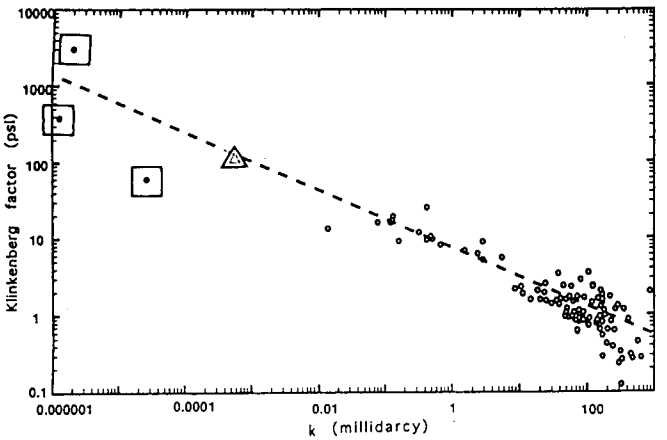

Figure 6. Klinkenberg b values plotted against permeability. Solid points in squares are these data, triangle is point from Reda (1987), and all other points and correlation line are from Jones (1972).

Correlation of hydrologic properties with rock mineralogy and texture. The four metagraywacke cores utilized for this investigation are very similar mineralogically and texturally. The principal but subtle mineralogic differences are slightly more expandable (smectite-bearing) illitic clay and a few per cent more disseminated pyrite in the three caprock cores relative to the reservoir core. Neither of these mineralogic variations is strongly correlated with either porosity or permeability. The measured porosities are fairly consistent about 2% no matter what the mineralogy (Table 2), and the two highest permeability values were recorded in a caprock and reservoir sample. These two most permeable samples share a common feature, however -- they are disrupted by late-stage microfractures. We cannot determine from these samples when the fractures formed. They could be natural reservoir features, but in the apparent absence of any fracture-filling or -coating secondary minerals, they could also be artifacts developed during cooling of the cores from reservoir to ambient temperatures.

The throughgoing veins believed to be possible fluid-flow channels in plug 15-2 were shown by subsequent microscopic examination to be fully filled by secondary minerals, supporting the idea that the flow was actually along younger microfractures. These microfractures, however, are seen in thin section to have apertures averaging <10 microns, with a maximum of 200 microns. This is far greater than the effective aperture of 1.6 μm (i.e., the aperture in a parallel plate fracture with the same transmissivity). In a fracture with spatially-varying aperture, however, asperities and flow restrictions influence the transmissivity disproportionately, so these data are not necessarily inconsistent. The fractures may also have closed under confining pressure (500 psi effective stress) during the permeability measurements.

CONCLUSIONS

1. Permeability measurements were made on three plugs from the caprock and one from the steam reservoir. Late-stage microfractures present in two of the plugs contributed to greater permeability, but the values measured for the two other plugs indicate that a typical value for matrix permeability is 1 to 2 x 10^{-21} m^2.

2. Klinkenberg slip factor *b* measured for these plugs are generally consistent with the inverse relationship between slip factor and permeability that Jones (1972) observed for plugs of much more permeable material.

3. The caprock and reservoir samples are nearly identical metagraywackes with only slight mineralogical differences which appear to have little influence on the rocks' measured hydrologic properties.

4. Late stage microfractures contributed to permeability of two of these samples but are suspected of being artifacts.

5. Capillary pressure curves measured for three cores were fit by power-law relationships. These relationships can be used to estimate relative permeability curves for the matrix rocks.

ACKNOWLEDGMENT

This work was supported by the U.S. Department of Energy, Assistant Secretary for Energy Efficiency and Renewable Energy, Geothermal Division; under Contract Nos. DE-AC03-76SF00098 and DE-AC07-95ID13274. Said support does not constitute an

endorsement of the views expressed in this paper. Thanks are due to Stefan Finsterle for data inversion using ITOUGH, to Sanjay Gangadhara and Charles Wei for conducting the experiments and for data analysis, and to our colleagues Karsten Pruess and Christine Doughty for careful reviews of the manuscript.

REFERENCES

Acheson, D.T., Vapor Pressure of Saturated Aqueous Salt Solutions, Humidity and Moisture, Fundamentals and Standards, A. Wexler and W.A. Wildhack eds., Reinhold Publishing Co., NYC, 1965, 3, 521–530.

Calhoun Jr., J.C., Lewis Jr., M., and Newman, R.C., Experiments on the Capillary Properties of Porous Solids, *Petroleum Transactions, AIME*, July 1949, 189–196.

Finsterle, S., and K. Pruess, Solving the Estimation-Identification Problem in Two-Phase Flow Modeling, *Water Resources Res. 31* (4), 913-924, 1995.

Gunderson, R.P. , Reservoir matrix porosity at The Geysers from core measurements. *Geothermal Resources Council, Transactions 14*, 1661-1665, 1990.

Hulen, J.B., and Nielson, D.L., 1995, Hydrothermal factors in porosity evolution and caprock formation at The Geysers steam field, California -- Insight from The Geysers Coring Project: Stanford University, 20th Workshop on Geothermal Reservoir Engineering, Proceedings, p. 91-98.

Hulen, J.B., Koenig, B.A., and Nielson, D.L., The Geysers Coring Project, Sonoma County, California -- Summary and initial results: Florence, Italy, World Geothermal Congress, Proceedings, p. 1415-1420, 1995.

Jones, S.C. A Rapid Accurate Unsteady-State Klinkenberg Permeameter *SPE Journal*, October 1972, 383-397.

Klinkenberg L.J., "The Permeability of Porous Media to Liquids and Gases," *Drill. and Prod. Prac.*, API 1941., p. 200-213.

Moore, J.N., and Gunderson, R.P., Fluid-inclusion and isotopic systematics of an evolving magmatic-hydrothermal system: *Geochimica et Cosmochimica Acta 59*, 3887-3907 , 1995.

Ning, X., The Measurement of Matrix and Fracture Properties in Naturally Fractured Low Permeability Cores Using a Pressure Pulse Method, Ph.D. Thesis, Texas A&M, December 1992, published as Gas Research Institute Report GRI-93/0103, March 1993.

Persoff, P. and Pruess, K. Two-Phase Flow Visualization and Relative Permeability Measurement in Natural Rough-Walled Rock Fractures, *Water Resources Res. 31* (5), 1175-1186, 1995 (Lawrence Berkeley Laboratory report LBL-35279).

Pruess, K., and O'Sullivan, M., Effects of Capillarity and Vapor Adsorption in the Depletion of Vapor–Dominated Geothermal Reservoirs, Proceedings 17th Workshop on Geothermal Reservoir Engineering, Stanford University, 165-174 (Lawrence Berkeley Laboratory report LBL–31692), 1992.

Reda, D.C. Slip-Flow Experiments in Welded Tuff: The Knudsen Diffusion Problem, in *Coupled Processesd Associated with Nuclear Waste Repositories*,, C.F. Tsang (ed.), Academic Press, New York, 485-493, 1987.

Ward, J.S., and Morrow, N.R., Capillary Pressures and Gas Relative Permeabilities of Low–Permeability Sandstone, *SPE Formation Evaluation*, September 1987, 345–356.